Immunology Letters 208 (2019) 52–59

Contents lists available at ScienceDirect

Immunology Letters

journal homepage: www.elsevier.com/locate/immlet

Identification of a neoantigen epitope in a melanoma patient with good response to anti-PD-1 antibody therapy

Chizu Nonomura[a,1], Masaki Otsuka[a,e,1], Ryota Kondou[a], Akira Iizuka[a], Haruo Miyata[a], Tadashi Ashizawa[a], Naoki Sakura[b], Shusuke Yoshikawa[e], Yoshio Kiyohara[e], Keiichi Ohshima[b], Kenichi Urakami[c], Takeshi Nagashima[c,h], Sumiko Ohnami[c], Masatoshi Kusuhara[d], Koichi Mitsuya[f], Nakamasa Hayashi[f], Yoko Nakasu[f], Tohru Mochizuki[b], Ken Yamaguchi[g], Yasuto Akiyama[a,*]

[a] Immunotherapy Division, Shizuoka Cancer Center Research Institute, 1007 Shimonagakubo, Nagaizumi-cho, Sunto-gun, Shizuoka 411-8777, Japan
[b] Medical Genetics Division, Shizuoka Cancer Center Research Institute, 1007 Shimonagakubo, Nagaizumi-cho, Sunto-gun, Shizuoka 411-8777, Japan
[c] Cancer Diagnostics Research Division, Shizuoka Cancer Center Research Institute, 1007 Shimonagakubo, Nagaizumi-cho, Sunto-gun, Shizuoka 411-8777, Japan
[d] Regional Resources Division, Shizuoka Cancer Center Research Institute, 1007 Shimonagakubo, Nagaizumi-cho, Sunto-gun, Shizuoka 411-8777, Japan
[e] Division of Dermatology, Shizuoka Cancer Center Hospital, 1007 Shimonagakubo, Nagaizumi-cho, Sunto-gun, Shizuoka 411-8777, Japan
[f] Division of Neurosurgery, Shizuoka Cancer Center Hospital, 1007 Shimonagakubo, Nagaizumi-cho, Sunto-gun, Shizuoka 411-8777, Japan
[g] Office of the President, Shizuoka Cancer Center Hospital, 1007 Shimonagakubo, Nagaizumi-cho, Sunto-gun, Shizuoka 411-8777, Japan
[h] SRL Inc., Shinjuku-ku, Tokyo 163-0409, Japan

ARTICLE INFO

Keywords:
Whole exome sequencing (WES)
Single nucleotide variant (SNV)
Mutant neoantigen
Tumor-infiltrating lymphocyte (TIL)
Single-cell RNA sequencing

ABSTRACT

Recent advances in next-generation sequencing have enabled rapid and efficient evaluation of the mutational landscape of cancers. As a result, many cancer-specific neoantigens, which can generate antitumor cytotoxic T-cells inside tumors, have been identified. Previously, we reported a metastatic melanoma case with high tumor mutation burden, who obtained complete remission after anti-PD-1 therapy and surgical resection. The rib metastatic lesion, which was used for whole-exome sequencing and gene expression profiling in the HOPE project, showed upregulated expression of PD-L1 mRNA and a high single-nucleotide variants number of 2712.

In the current study, we focused on a metastatic melanoma case and candidate epitopes among nonsynonymous mutant neoantigens of 1348 variants were investigated using a peptide-HLA binding algorithm, *in vitro* cytotoxic T-cell induction assay and HLA tetramer staining. Specifically, from mutant neoantigen data, a total of 21,066 9-mer mutant epitope candidates including a mutated amino acid anywhere in the sequence were applied to the NetMHC binding prediction algorithm. From *in silico* data, we identified the top 26 mutant epitopes with strong-binding capacity. A cytotoxic T-cell induction assay using 5 cancer patient-derived PBMCs revealed that the mutant ARMT1 peptide sequence (FYGKTILWF) with HLA-A*2402 restriction was an efficient neoantigen, which was detected at a frequency of approximately 0.04% in the HLA-A24 tetramer stain. The present success in identifying a novel mutant antigen epitope might be applied to clinical neoantigen screening in the context of an NGS-equipped medical facility for the development of the next-generation neoantigen cancer vaccines.

1. Introduction

Many cancers feature the accumulation of mutations, including exonic single-nucleotide variants (SNV) comprising nonsynonymous, nonsense, indel and frame-shift mutations. Nonsynonymous mutations largely account for the SNVs identified in cancers, which are generally classified into two types; 1) driver mutations that activate cancer cell signaling and lead to uncontrolled cell growth and tumor metastasis, and 2) passenger mutations that may not contribute to the tumorigenic phenotype, but increase immunogenicity [1–3].

Abbreviations: WES, whole exome sequencing; GEP, gene expression profiling; TMB, tumor mutation burden; HLA, human leukocyte antigen; DC, dendritic cell; CTL, cytotoxic T cell; PBMC, peripheral blood mononuclear cell; CMV, cytomegalovirus

* Corresponding author at: Immunotherapy Division, Shizuoka Cancer Center Research Institute, 1007 Shimonagakubo, Nagaizumi-cho, Sunto-gun, Shizuoka 411-8777, Japan.
E-mail address: y.akiyama@scchr.jp (Y. Akiyama).
[1] These authors contributed equally to this work.

https://doi.org/10.1016/j.imlet.2019.02.004
Received 29 October 2018; Received in revised form 19 February 2019; Accepted 26 February 2019
Available online 14 March 2019

Recent advances in next-generation sequencing (NGS) have promoted the rapid evaluation of the mutational landscape of human cancers and have strongly accelerated the development of novel neoantigens that can be presented by HLA protein as mutant peptide and induce potent cytotoxic T-cells that can recognize the single amino acid difference between mutated and nonmutated peptides [4–6]. Additionally, NGS technology has revealed some cancers with very high tumor mutation burdens (TMBs), such as melanoma, non-small cell lung and colorectal cancers, which have shown more than 500 SNVs or 20 TMBs [7–10]. Furthermore, regarding the profiling of neoantigens, Schumacher et al., using genome data of more than 20,000 tumors, demonstrated that the frequency of identified neoantigens was less than 0.1% and that CD8 T-cell neoantigen epitopes were derived from oncogene (8%) and passenger mutations (92%), whereas CD4 T-cell epitopes were all derived from passenger mutations [11].

In our HOPE project, which launched in 2014 and reached more than 3000 tumor patients registered and analyzed using whole exome sequencing (WES) and gene expression profiling (GEP), we identified approximately 5% of hypermutator tumors with more than 500 SNVs in 3042 cases and verified that hypermutation was associated with PD-L1 gene expression level [12–15].

In the current study, we focus on a metastatic melanoma case with high tumor mutation burden (2712 SNVs), that obtained complete remission after anti-PD-1 therapy and surgical resection [16] and investigated candidate epitopes among nonsynonymous mutant neoantigens of 1348 variants using a peptide-HLA binding algorithm, *in vitro* cytotoxic T-cell induction assay and HLA tetramer staining.

2. Materials and methods

2.1. Reagents and cell lines

Recombinant human (rh) granulocyte macrophage colony-stimulating factor (GM-CSF), rh-IL-1β, rhIL-2, rhIL-4, rhIL-7, and tumor necrosis factor (TNF)-α were purchased from Pepro Tech Inc. (Rocky Hill, NJ). Interferon (IFN)-α and IFN-γ were purchased from Sumitomo and Shionogi Pharmaceutical Co, Ltd., Japan, respectively. Poly I/C was obtained from Amersham Biosciences Corp. (Piscataway, NJ). TISI and T2-A24 cells were used as target cells for the IFN-γ production assay and *in vitro* CTL stimulation, respectively.

2.2. Project HOPE at the Shizuoka cancer center

Project HOPE (High-tech Omics-based Patient Evaluation) was conducted in accordance with the Ethical Guidelines for Human Genome and Genetic Analysis Research and the study was approved by the Institutional Review Board of the Shizuoka Cancer Center (SCC), Japan. Comprehensive whole-exome sequencing (WES) with next-generation sequencers and gene expression profiling (GEP) with DNA microarray were performed using cancer tissues and PBMCs from 3052 registered cancer patients. Among them, 13 melanoma patients were registered and characterized using multiomics analyses, including next-generation sequencing (NGS).

In the current study, we focus on a metastatic melanoma case (MEL-HOPE002) with high tumor mutation burden (2712 SNVs), which achieved a complete remission after anti-PD-1 therapy and surgical resection, and investigated candidate epitopes among nonsynonymous mutant neoantigens of 1348 variants using a peptide-HLA binding algorithm, *in vitro* cytotoxic T-cell induction assay and HLA tetramer staining.

2.3. GEP analysis

GEP was performed using SurePrint G3 Human GE 8 × 60 K v2.0 arrays (Agilent Technologies, Santa Clara, CA, USA) as previously reported [15]. Briefly, signal data analysis was performed using GeneSpring version 13.1.1 software (Agilent Technologies). Raw signal intensity values in tumor were log transformed and normalized to the 75th percentile.

2.4. WES analysis and Sanger sequencing

WES and variant calling were performed using the Ion Proton AmpliSeq Exome kit and the Ion Torrent server as previously reported [12]. Briefly, all variants called by the variant caller were available. However, the data presented in SCC represent those variants considered to be of good quality, based on filtering: sequences with quality < 30, frequency < 10% or coverage < 20 were discarded. After filtering a second time to remove germline variants (using data from dbSNP, the 1000 Genomes Project), the obtained sequence data were likely somatic. Single-nucleotide variants (SNVs) of the total exonic mutations for each sequenced tumor included nonsynonymous, synonymous, and indels/frameshift mutations.

Sanger sequencing of PCR products was performed using a microcapillary DNA sequencer (Thermo Fisher Scientific, Waltham, CA, USA). Acidic residue methyltransferase-1 (ARMT1)-specific PCR primers were synthesized by Invitrogen Inc. (Waltham, CA, USA). Tumor-derived total RNA was extracted from FFPE sections from the MEL-HOPE002 case using a High Pure FFPE RNA Micro kit (Roche, Molecular Biochemicals, Mannheim, Germany). Reverse transcription was performed with SuperScript™ III Reverse Transcriptase and random hexamers (Thermo Fisher Scientific, Waltham, CA, USA). PCR reactions were performed using the Ex Taq Hot Start Version (Takara Bio Inc., Seta, Shiga, Japan) and ARMT1-specific primers (forward primer: 5′-TGAGGTTCATTTTTATGGAA-3′; reverse primer: 5′-CCAGTCAGCCC CACACTT-3′). For sequencing, the forward primer was used. PCRs were performed using the following conditions: initial PCR activation step at 94 °C for 2 min; 45 cycles of denaturation at 98 °C for 10 s, annealing at 55 °C for 30 s and extension at 72 °C for 30 s; and a final extension step at 72 °C for 4 min.

2.5. HLA-binding prediction algorithm

The HLA-typing of the melanoma case in question was A*2402/2402. Nonsynonymous mutations of 1348 variants from 1344 different genes were collected, and 17 amino acid sequences, including 8 forward and 8 backward amino acids from mutated amino acids, were identified from 9 sets of 9-mer sequence containing mutated amino acid from each mutated gene. A total of 12,066 candidate sequences were applied to the HLA-binding prediction algorithm, NetMHC4.0 (http://www.cbs.dtu.dk/services/NetMHC/). The HLA-A*2402-restricted sequence candidates with strong binding capacity (< 50 nM) were selected and evaluated for synthetic peptide candidates.

2.6. In silico HLA-A24 protein-peptide docking program

Briefly, to build the initial 3D structure of any given A24-restricted epitope candidate peptide, we established HLA-A24-peptide docking simulation software using MODELLER (version 9v5) and AutoDock (version 4.0). Thus, we predicted the affinity between HLA-A24 and neoantigen candidate peptides. The method to evaluate the docking activity was described previously [17].

2.7. Peptide synthesis

Twenty-four HLA-A*2402-restricted sequence candidates with strong binding capacity (< 50 nM) were selected for chemical synthesis using the method reported previously [17] in our research institute. The HLA-A24-restricted CMVpp65$_{341\text{-}349}$ (QYDPVAALF) was used as a positive control.

2.8. CTL induction assay and tetramer staining

Cultures of PBMCs from five HLA-A*2402$^+$ cancer patients (GB-SCC017, 019, 024, 025 and 026) and three HLA-A*2402$^+$ healthy volunteers were used for *in vitro* CTL induction. The clinical research using PBMCs was approved by the Institutional Review Board of Shizuoka Cancer Center, Shizuoka, Japan. CTL induction cultures were described previously [17]. Briefly, PBMCs were incubated in 6-well culture plates (Corning Inc., Corning, NY, USA) at 4×10^6 cells/ml in RPMI1640 medium supplemented with L-glutamine (2 mM), penicillin (100 U/ml), streptomycin (100 U/ml) and 5% FBS for 90 min. After the incubation, the non-adherent cells were removed and the adherent monocyte-enriched population was cultured in the presence of 40 ng/ml of GM-CSF and 40 ng/ml of IL-4. A combination of maturation cytokines, such as TNF-α (50 ng/ml), IL-1β (25 ng/ml), IFN-α (3000 U/ml), IFN-γ (1000 U/ml), and poly I/C (20 μg/ml) was added on day5 of culture. After 7 days culture, most dendritic cells (DC) were positive for maturation markers like CD83, CD80, CD86, CD11c and HLA-DR in FACS analysis (data not shown). Harvested DC were suspended with Dulbecco's PBS with calcium and magnesium [referred to as PBS(+)] containing 1% human serum albumin (CSL Behring LLC, Kankakee, IL, USA) and incubated with various HLA-A24 peptides (each final 25 μg/ml) for 2 h at 37°C. DC were irradiated (30 Gy) and incubated with non-adherent autologous PBMC at a ratio of 1:50-100 in the presence of 10 ng/ml of IL-7. After 7 day culture, the PBMC were re-stimulated with irradiated same peptide-pulsed DC and incubated for a week. Human IL-2 was added to PBMC cultures every 2–3 days at a final dose of 2.5 ng/ml. After 2 rounds of *in vitro* DC stimulation, PMBC were utilized for IFN-γ production assay. For HLA-A24 tetramer staining, CTLs after 2 rounds of mature DC stimulation were cocultured with HLA-A24 peptide-pulsed T2-A24 cells at the ratio of 10:1 and were used for tetramer staining in the presence of FITC anti-CD8 antibody.

2.9. IFN-γ production assay

TISI cells were incubated with HLA-A24 neoantigen peptides overnight at 20 μg/ml suspended in PBS(+) containing 1% HSA and used as target cells. Cultured PBMC (1×10^5) and HLA-A24 peptide-pulsed TISI cells (1×10^5) were co-incubated in a round bottomed-96-well microculture plate for 24 h. Finally, supernatants were collected and IFN-γ levels were measured using an ELISA kit specific for human IFN-γ (Biosource, Camallilo, CA).

2.10. Immunohistochemistry analysis of ARMT1 protein

For ARMT1 protein staining, rabbit anti-human ARMT1 polyclonal antibody was purchased (Atlas Antibodies AB, Bromma, Sweden) and used for immunohistochemistry (IHC) analysis.

2.11. Neoantigen-specific T-cell receptor gene repertoire analysis by human TCR α/β profiling kit

A total of 715 ARMT1-A24 tetramer$^+$ CTLs were sorted and applied to Switching Mechanisms at 5' End of RNA Template (SMARTer™) human TCR α/β profiling kit (Clontech Laboratories Inc., Mountain View, CA, USA). Briefly, first-strand cDNA synthesis is dT-primed (using TCR-dT Primer) and performed by the MMLV-derived SMARTScribe™ Reverse Transcriptase (RT), which adds nontemplated nucleotides sequence upon reaching the 5′ end of each mRNA template. This additional sequence, referred to as "SMART sequence", serves as a primer-annealing site for subsequent rounds of PCR. Following RT, two rounds of PCR are performed in succession to amplify cDNA sequences corresponding to variable regions of TCR-α and/or TCR-β transcripts. Following post-PCR purification, size selection and quality analysis, the library is available for MiSeq NGS analysis (Illumina, San Diego, CA, USA). TCR repertoire analysis was performed based on hypervariable VDJ segment sequencing using MiTCR, software for T-cell receptor sequencing data analysis, which is available from http://mitcr.milaboratory.com/.

2.12. Neoantigen-specific T-cell receptor gene repertoire analysis by single-cell RNA sequencing

Approximately 230 ARMT1-A24 tetramer$^+$ T cells and 5900 CMV-A24 tetramer$^+$ T cells as a positive control were sorted and applied to the Chromium™ single-cell controller (10x Genomics, Inc., Pleasanton, CA, USA) using the Chromium™ single cell 3` v2 reagent kit containing a chip for the efficient capture of single cells. Single- cell partitioning, lysis and barcoding were performed on the tip using rapid and efficient microfluidics technology, resulting in a high-quality library of RNA fragments. The library was sequenced using MiSeq NGS (Illumina, San Diego, CA, USA) and TCR repertoire analysis was performed based on hypervariable VDJ segment sequencing using Cell Ranger™ informatics and Loupe Cell and VDJ Browser™ visualization software programs.

2.13. Statistical analysis

Statistical differences were analyzed using Student's t-test. Values of $P < 0.05$ were considered statistically significant.

3. Results

3.1. Selection of mutated neoantigen candidate peptides

From the data containing 1348 nonsynonymous mutant sequences, a total of 21,066 9-mer mutant epitope candidates including a mutated amino acid anywhere in the sequence were applied to the NetMHC binding prediction algorithm. HLA-A*2402-restricted 26 mutant peptide sequences with strong binding affinity (< 50 nM) were detected, and after *in silico* screening using HLA-A24-peptide docking simulation software, 24 mutant peptides were ultimately verified as neoantigen candidates and were chemically synthesized (Fig. 1, Table 1).

3.2. Expression levels of mutant genes and Sanger resequencing

GEP analysis revealed that 4 genes, PSMD6, TMEM45A, ARMT1 and FBXO46, showed positive expression in MEL-HOPE-002 case (Supplementary Table 1). The specific base replacements were confirmed using Sanger sequencing (Fig. 2) in the 4 mutant genes, which identified the following amino acid substitutions: S274 L in the PSMD6 gene, N239 K in the TMEM45A gene, P286 L in the ARMT1 gene and R450W in the FBXO46 gene.

3.3. CTL induction assay and tetramer staining

PBMCs from five HLA-A*2402$^+$ cancer patients (GB-SCC017, 019, 024, 025 and 026) were used for *in vitro* CTL induction. Five cancer patients-derived PBMCs were used for the 1st screening assay testing all 24 peptides. Regarding the 1 st screening, GB-SCC019 and 025 responded to no peptides, but other 3 cases responded to any YA7,8,14 and 25 peptides. The two more screening assay using GB-SCC017, 024 and 026 PBMCs, and 4 hit peptides, were performed. Eventually, only GB-SCC024 PBMC-derived CTLs showed reproducibly higher IFN-γ production against ARMT1 mutant peptide (Supplementary Fig. S1, Fig. 3A). However, GB-SCC024 PBMCs-derived CTLs did not respond to ARMT1 wild type peptide (Fig. 3B). Additionally, three PBMCs derived from healthy volunteers with HLA-A*2402 typing (VOL-1, 2 and 3) responded to neither YA14 mutant nor YA14 wild-type pepride-treated target cells (Fig. 3C).

For ARMT1 mutant peptide-tetramer staining, GB-SCC024 CTLs stimulated with 2 rounds of mature DCs and 1-time HLA-A24 T2 cells treated with mutant ARMT1 peptide were stained using FITC-anti-CD8

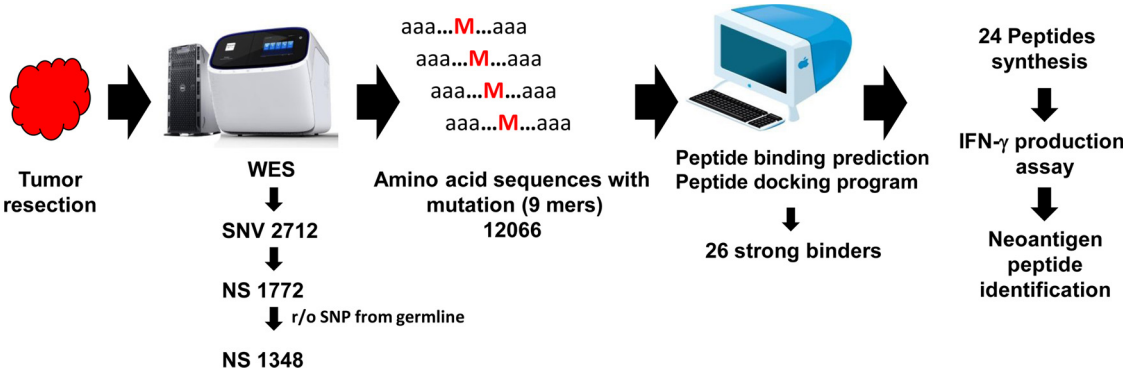

Fig. 1. Platform for the melanoma neoantigen screening procedures. A metastatic melanoma tumor exhibited a high number of mutations (SNV 2712), and after exclusion of germ line SNPs, 1348 nonsynonymous mutations were investigated for neoantigen screening. Through *in silico* binding affinity screening of 12,066 amino acid fragments with mutations, 26 strong binders were selected. Ultimately, 24 neoantigen peptides candidate were synthesized and used for CTL assay (IFN-γ production), and one neoantigen peptide was identified.

antibody and APC-HLA-A24 ARMT1 tetramer. As a result, HLA-A24 ARMT1 and CMV tetramer-positive $CD8^+$ T cells were identified in 0.04% and 0.15%, respectively, of cultured CTLs (Fig. 4). A total of 715 sorted $CD8^+$ARMT1 $tetramer^+$ T cells were used for TCR gene repertoire analysis using human TCR α/β profiling kit. Meanwhile, a total of 5900 CMV-A24 $tetramer^+$ T cells were for TCR analysis using single-cell RNA sequencing.

3.4. Immunohistochemistry analysis of ARMT1 protein in metastatic melanoma

Melanoma cells were partially positively stained at nuclear membranes with anti-ARMT1 polyclonal antibody (Fig. 5).

3.5. TCR repertoire identification using NGS

After sorting the mutant ARMT1 tetramer-positive or CMV tetramer-positive cell populations, TCR sequencing was performed using NGS. The TCR sequence data obtained with a human TCR α/β profiling (SMARTer™) kit and a single-cell RNA sequencing method (Chromium™) are shown (Table 2). TCR analysis of mutant ARMT1 tetramer-positive T cells in bulk using the SMARTer kit showed that major variable allele clones with more than 10% frequency were identified in the TCR-α and TCR-β repertoires, TRAV24*01 and TRBV5-6*01, respectively (Table 2A). TCR analysis of mutant ARMT1 tetramer-positive T cells *via* single-cell RNA sequencing using Chromium™ was not successful because of very small number of cells analyzed. However, TCR analysis of CMV tetramer-positive T cells indicated that the most common single-cell clone with the TRAV24 and TRBV5-1 pair was 48% (Table 2B).

Table 1
Neoantigen candidate peptide list.

Peptide name	Gene name	Position[a]	Peptide	Affinity(nM)	Bind level[b]	Meand G[c] (kcal/mol)
YA24-TMEM178B	TMEM178B	1	RYPRYLYKL	10.3	SB	3.74
YA1-MMP2	MMP2	4	EYCKFSFLF	12.7	SB	−6.83
YA4-DNAH12	DNAH12	6	WYLKVINLF	12.8	SB	−3.75
YA12-PSMD6	PSMD6	1	RYSVFFQLL	13.6	SB	−1.03
YA25-MAS1	MAS1	1	LYYEYWSNF	15.7	SB	1.11
YA3-TRPA1	TRPA1	1	KYLQCPLKF	16.6	SB	−4.68
YA2-OR4A5	OR4A5	3	IYVRPFSNF	16.8	SB	−7.13
YA6-PDGFRA	PDGFRA	3	SYEKIYLDF	20.3	SB	−4.06
YA9-GABRQ	GABRQ	1	SYGVRFNSF	20.7	SB	−3.94
YA7-TMEM45A	TMEM45A	8	KYAFITWLV	22.2	SB	−4.63
YA10-SLAIN1	SLAIN1	0	YYSPQAQTL	24.4	SB	−4.12
YA26-IL12B	IL12B	2	TWSTPHFYF	26.9	SB	−9.61
YA27-CLDN10	CLDN10	7	FYCRPHFTI	28.1	SB	1.4
YA15-UNC13C	UNC13C	2	TYGESFHII	29.2	SB	−3.64
YA28-OR5M11	OR5M11	7	RFHTPMYFF	29.8	SB	−1.87
YA5-SCN3A	SCN3A	3	LMMSLSALF	33.0	SB	−7.9
YA8-SLC26A7	SLC26A7	1	PYISGPLRF	33.1	SB	−7.74
YA13-TRRAP	TRRAP	2	IYLLQYVTL	34.6	SB	−5.88
ND	HTR2C	3	NYFLMYLAI	35.7	SB	1.27
YA17-CAPN9	CAPN9	1	QWINLFLQF	36.4	SB	−2.43
YA11-TTC21B	TTC21B	6	LYNAGLFLW	36.7	SB	−8.75
YA14-ARMT1	ARMT1	2	FYGKTILWF	40.5	SB	−7.19
YA29-IL13RA2	IL13RA2	8	LLPPVYLTF	43.0	SB	−2.81
YA30-FBXO46	FBXO46	6	LYWHVSHDF	43.1	SB	3.38
YA16-HTR2C	HTR2C	7	IYIGVSVPI	47.7	SB	−6.85
ND	LOC650293	2	YYKIVTYIL	49.4	SB	−1.76

ND: not done.
[a] Position: the position of mutated amino acid.
[b] Bind level: affinity less than 50 nM indicates strong binding.
[c] dG: in peptide-docking assay using algorithm, an affinity was calculated as the Gibbs free energy of (deltaG).

Gene name	Gene ID	Gene symbol	SnpEff prediction	Sequence
acidic residue methyltransferase 1	79624	ARMT1	missense:cCa/cTa:P167L,P286L	VHFYGKTILWFVSDTTI

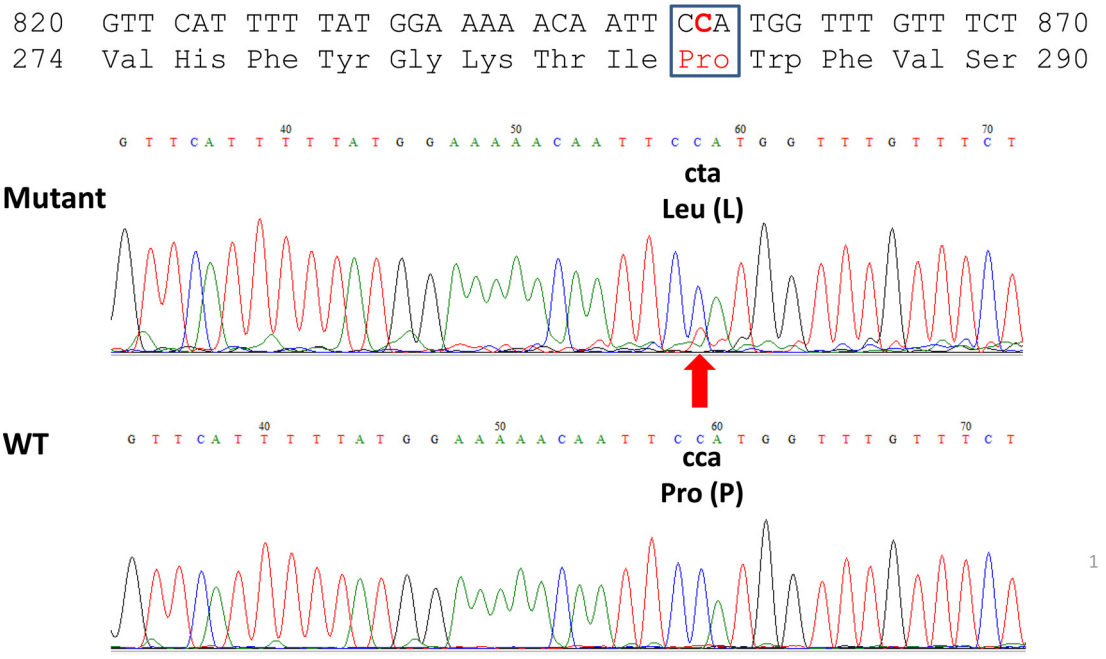

Fig. 2. Confirmation of the ARMT1 mutation using Sanger sequencing. The missense: cca/cta: P286L was successfully identified.

4. Discussion

Based on the successful achievement of immune checkpoint blockade for PD-1/PD-L1 in the clinical trials, positive PD-L1 expression, high mutation burden and microsatellite instability (MSI) high status are considered to be possible biomarkers for clinical responder prediction and good prognosis in melanoma, non-small cell lung cancer and colon cancer patients treated with PD-1/PD-L1 blockade [7,8,18]. Moreover, tumor-infiltrating lymphocyte (TIL) or $CD8^+$ T cells as tumor microenvironment (TME) factor becomes more important parameters for determining good antitumor response and prognosis of cancer patients [19,20].

Associated with high mutation load in cancer patients with good responses to the immune checkpoint blockade, mutated cancer antigens, so-called neoantigens, have been intensively focused upon and investigated as cancer rejection antigens [21–24]. The specific mechanism responsible for hypermutation is demonstrated as a mutation signature, such as the APOBEC family [25], meanwhile the elegant and efficient technologies that enable us to identify a variety of neoantigens have also been developed [26–31]. At first, *in vivo* model bearing mouse tumors demonstrated that tumor-derived neoantigens could be identified and could trigger the efficient induction of cytotoxic T-cells against cancers [4–6]. In parallel with the advance in NGS, many clinical studies have investigated the neoantigen profiling over a broad range of cancers treated or not treated with immune checkpoint blockade. In addition to NGS technology, proteomics-based technology was developed and has been successfully applied to the identification of neoantigen candidate peptide sequences [32]. Interestingly, Kochin et al. [32] established the procedure to isolate detergent-solubilized peptide-HLA-A24 complexes from MSI-high colon cancer cell lines using protein A-sepharose beads linked to anti-HLA-A24 monoclonal antibody (C7709A2) and eventually identified HLA-A24-restricted peptides by LC–MS/MS analysis. This technology contributes a novel approach and can be an alternative way to detect neoantigen candidate besides NGS methods.

In the current study, we also successfully identified functional HLA-A24-restricted neoantigen peptides using NGS-based exome sequencing, *in silico* programs and *in vitro* immunological assays. Importantly, we have tried to determine the TCR repertoire CDR3 sequence from tetramer-positive single cells using single-cell TCR RNA-sequencing. Single-cell RNA-sequencing is a recently-developed advanced technology based on microfluidics and the NGS sequencing platform and, to date, has been frequently applied to cancer exome sequencing and has indicated heterogeneity in tumor tissues [33–37]. A few clinical studies investigating the TCR repertoire from TIL or peripheral blood cells of cancer patients have been demonstrated thus far and more evidence for TCR repertoire and functional classification of TILs has been accumulated [38–40]. Recently, Tirosh et al. applied single-cell RNA-sequencing analysis to cancerous and immune cells from melanoma patients and demonstrated a T cell exhaustion signature and their connection to T cell activation, and concluded that single-cell RNA sequencing is an efficient tool for analyzing TCR repertoire profiling [38]. Additionally, Zheng et al. reported successfully performing deep single-cell TCR RNA sequencing on 5063 T cells isolated from peripheral blood and tumor from hepatocellular cancer patients and identified 11 T cell subsets based on their molecular and functional properties [39].

We identified specific TCR CDR3 sequence derived from ARMT-1 neoantigen peptide-HLA-A24 tetramer positive T cells (715 cells) using a human TCR α/β profiling kit. ARMT1, called C6orf211 is an enzyme that specifically targets proliferating cell nuclear antigen (PCNA) in breast cancer cells [41]. Additionally, three open reading frame (ORF) genes located immediately upstream (on 6q25.1) of ESR1, C6ORF96, C6ORF97 and C6ORF211 (ARMT-1) were highly correlated with ESR1 expression [42]. Thus, the ARMT-1 gene is considered to be involved in a breast cancer cell survival control mechanism mediated by the ESR-1 gene.

Finally, we have constructed a single-cell RNA sequencing platform combined with microfluidics and NGS technology, that will enable every clinical researcher to analyze TME biomarkers in terms of their genetic, phenotypic and even functional properties. This valuable

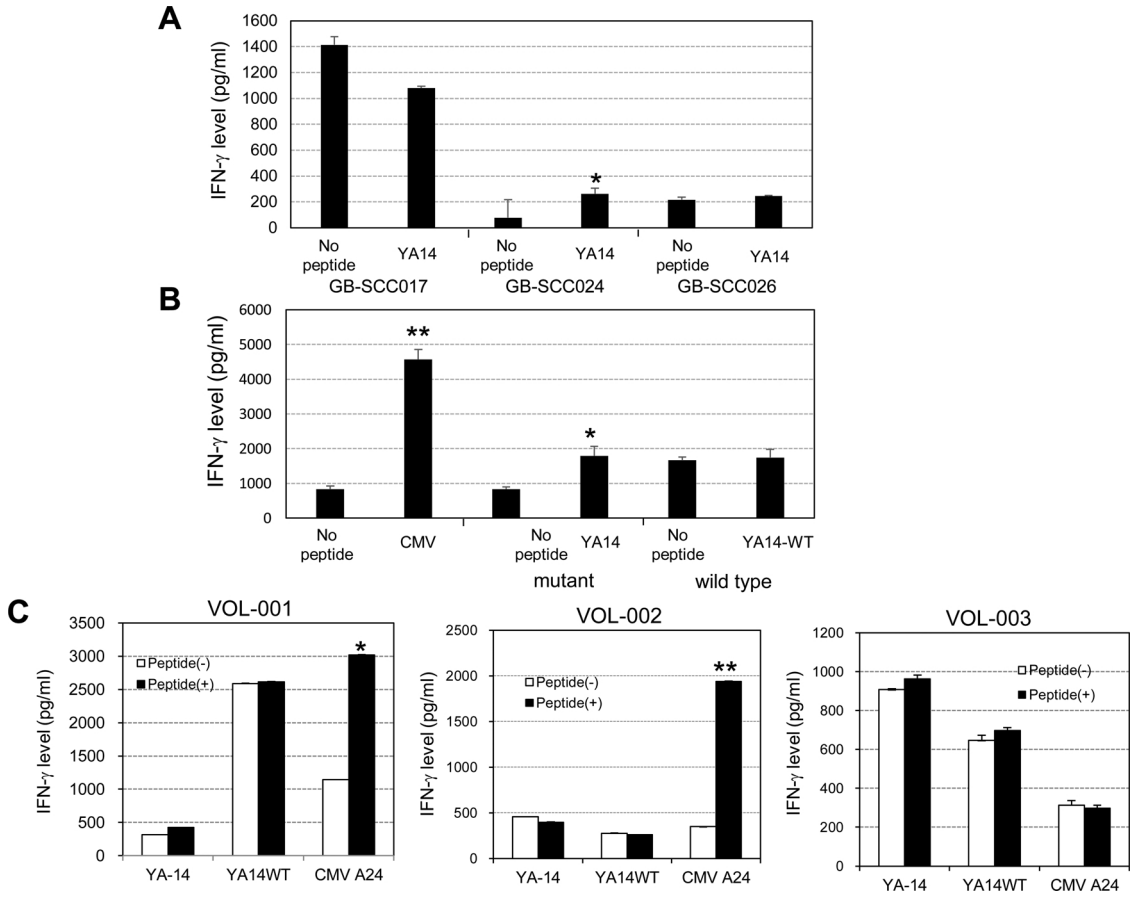

Fig. 3. CTL induction assay against neoantigen candidate peptides using cancer patients-derived PBMCs. (A) CTL induction activity of the YA14 neoantigen peptide (mutant ARMT1). The data show a representative of three CTL assay experiments using 3 cancer patients (GB-SCC017, GB-SCC024 and GB-SCC026)-derived PBMCs. (B) CTL induction activity of YA14 mutant peptide, YA14 wild type peptide and CMV pp65 peptide using GB-SCC024 PBMCs, and (C) three PBMCs derived from healthy volunteers. Each column shows the mean ± SD of triplicate assays. *; $P < 0.05$, **; $P < 0.01$, statistically significant.

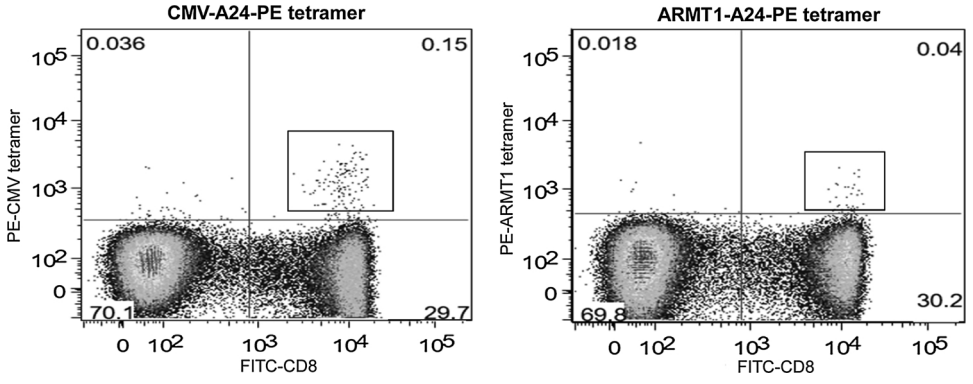

Fig. 4. Identification of ARMT1-specific $CD8^+$ T cells from GB-SCC024 PBMCs using tetramer staining. $CD8^+$ T cells cocultured with autologous DCs with mutated ARMT1 peptide were stained with HLA-A24 ARMT1-PE tetramer and $CD8^+$ARMT1 $tetramer^+$ CTLs were detected (0.04%). A total of 715 of sorted $CD8^+$ARMT1 $tetramer^+$ T cells were detected and were used for TCR gene repertoire analysis. CMVpp65-HLA-A24-PE tetramer was used as a positive control.

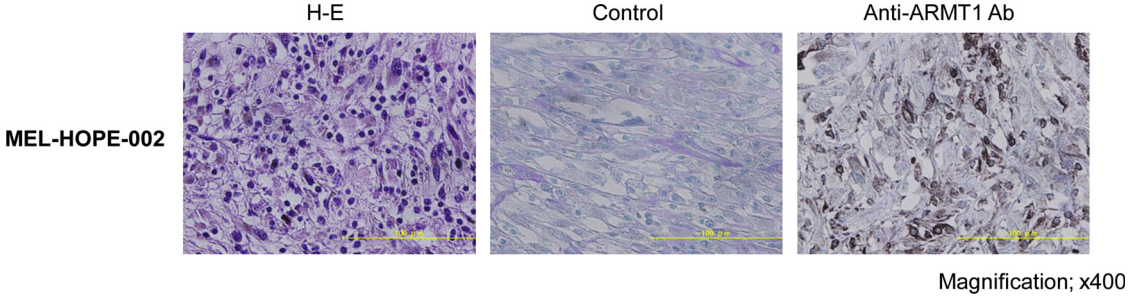

Fig. 5. ARMT1 protein expression in metastatic melanoma tumor from the MEL－HOPE002 case. For ARMT1 proteins staining, rabbit anti-human ARMT1 polyclonal antibody was used. Magnification; x 400.

Table 2
TCRa and TCRb CDR3 sequence from ARMT1- or CMVpp65-specific CD8+ T cells.

A

ARMT1-TCRα sequence (more than 5%)

	Read count	Percentage	CDR3 nucleotide sequence	CDR3 amino acid sequence	V alleles	J alleles
①	154542	34.7	TGTGCCTTTGCTGGTGGTACTAGCTATGGAAAGCTGACATTT	CAFAGGTSYGKLTF	TRAV24*01	TRAJ52*01
②	95225	21.4	TGTGCTGTGCAGGCTGGGAACTATGGTCAGAATTTTGTCTTT	CAVQAGNYGQNFVF	TRAV20*01	TRAJ26*01

ARMT1-TCRβ sequence (more than 5%)

	Read count	Percentage	CDR3 nucleotide sequence	CDR3 amino acid sequence	V alleles	J alleles
①	16655	16.5	TGTGCCAGCAGTCGCGGGACACTTCACTATGGCTACACCTTC	CASSRGTLHYGYTF	TRBV5-6*01	TRBJ1-2*01
②	7484	7.4	TGTGCCAGCAGCCTCGGACAGGGGATTGTAGCAATCAGCCCCAGCATTTT	CASSLGQG~CSNQPQHF	TRBV11-3*01	TRBJ1-5*01
③	6504	6.5	TGTGCCAGCAGCTTGGGGGCAGCTCCTCAAGAGACCCAGTACTTC	CASSLGAAPQETQYF	TRBV5-6*01	TRBJ2-5*01
④	6435	6.4	TGCGCCAGCAGCACCCGGGTGGTAGCGGGCAACAATGAGCAGTTCTTC	CASSTRVVAGNNEQFF	TRBV4-1*02, TRBV4-1*01	TRBJ2-1*01

B

CMVpp65-the TCRα and TCRβ pair sequence (more than 5%)

	Read count	Percentage	CDR3 nucleotide sequence	CDR3 amino acid sequence	V alleles	J alleles
①	835	47.7	TRA:TGTGCCCGTTCAACTGGGGCAAACAACCTCTTCTTT	TRA:CARSTGANNLFF	TRAV24	TRAJ36
			TRB:TGCGCCAGCAGCGATCCGGGACATCAATTATATGGCTACACCTTC	TRB:CASSDPGHQLYGYTF	TRBV5-1	TRBJ1-2
②	341	19.5	TRA:TGTGCCTCACCAGGGGCTGGTGGTACTAGCTATGGAAAGCTGACATTT	TRA:CASPGAGGTSYGKLTF	TRAV24	TRAJ52
			TRB:TGTGCCAGCAGCTTATATACCGCGGTGGAGACCCAGTACTTC	TRB:CASSLYTAVETQYF	TRBV7-8	TRBJ2-5
③	199	11.4	TRA:TGTGCCCGCCTCCATGGCTCTAGCAACACAGGCAAACTAATCTTT	TRA:CARLHGSSNTGKLIF	TRAV24	TRAJ37
			TRB:TGTGCCTGGAAATTCCGGGACAGTACCTACGAGCAGTACTTC	TRB:CAWKFRDSTYEQYF	TRBV30	TRBJ2-7
④	89	5.1	TRA:TGTGCCTCGCTAAGGGGGGCAAACAACCTCTTCTTT	TRA:CASLRGANNLFF	TRAV24	TRAJ36
			TRB:TGTGCCAGCAGCCCGCTAACAGCCACAGATACGCAGTATTTT	TRB:CASSPLTATDTQYF	TRBV7-8	TRBJ2-3

opportunity could be the next breakthrough in investigating tumor immunity biology, which has recently come under the spotlight because of immune checkpoint blockade therapy.

Author contributions

MO, CN and YA designed the study and drafted the manuscript. RK, AI, HM, TA and CN participated in the design of the experiments and performed the biological assays. NS and TM supplied synthetic peptides for biological assays. KM, NH, YN, YK and SY were responsible for supplying patient-derived materials for clinical research. KO, KU, TN and SO analyzed melanoma specimen and supplied the genomic data. MK and KY reviewed the manuscript. YA was responsible for organizing and completing the entire study. All authors read and approved the final draft.

Conflict of interest statement

The authors declare that they have no conflict of interest.

Acknowledgements

This work was supported by a grant to Yasuto Akiyama by JSPS KAKENHI (grant no. 17K07209), Japan.

Appendix A. Supplementary data

Supplementary material related to this article can be found, in the online version, at doi:https://doi.org/10.1016/j.imlet.2019.02.004.

References

[1] B. Vogelstein, N. Papadopoulos, V.E. Velculescu, S. Zhou, Doaz LA Jr, K.W. Kinzler, Cancer genome landscapes, Science 339 (2013) 1546–1558, https://doi.org/10.1126/science.1235122.
[2] S.A. Forbes, D. Beare, P. Gunasekaran, K. Leung, N. Bindal, H. Boutselakis, et al., COSMIC: exploring the world`s knowledge of somatic mutations in human cancer, Nucleic Acids Res. 43 (2015) D805–11, https://doi.org/10.1093/nar/gku1075 (Database issue).
[3] Y. Kawakami, T. Yaguchi, H. Sumimoto, C. Kudo-Saito, N. Tsukamoto, T. Iwata-Kajihara, et al., The Tumor Immunoenvironment, Springer Science+Buisiness Media, Dortrecht, 2013, pp. 307–323, https://doi.org/10.1007/978-94-007-6217-6_12.
[4] S. Kreiter, J.C. Castle, O. Tureci, U. Sahin, Targeting the tumor mutanome for personalized vaccination therapy, Oncoimmunology 1 (2012) 768–769, https://doi.org/10.4161/onci.19727.
[5] F. Duan, J. Duitama, S. Al Seesi, C.M. Ayres, S.A. Corcelli, A.P. Pawashe, et al., Genomic and nioinformatic profiling of mutational neoepitopes reveals new rules to predict anticancer immunogenicity, J. Exp. Med. 211 (2014) 2231–2248, https://doi.org/10.1084/jem.20141308.
[6] J.C. Castle, S. Kreiter, J. Diekmann, M. Löwer, N. van de Roemer, J. de Graaf, et al., Exploiting the mutanome for tumor vaccination, Cancer Res. 72 (2012) 1081–1091, https://doi.org/10.1158/0008-5472.CAN-11-3722.
[7] A. Snyder, V. Makarov, T. Merghoub, J. Yuan, J.M. Zaretsky, A. Desrichard, et al., Genetic basis for clinical response to CTLA-4 blockade in melanoma, N. Engl. J. Med. 371 (2015) 2189–2199, https://doi.org/10.1056/NEJMoa1406498.
[8] N.A. Rizvi, M.D. Hellmann, A. Snyder, P. Kvistborg, V. Makarov, J.J. Havel, et al., Mutational landscape determines sensitivity to PD-1 blockade in non-small cell lung cancer, Science 348 (2015) 124–128, https://doi.org/10.1126/science.aaa1348.
[9] R.J. Hause, C.C. Prichard, J. Shendure, S.J. Salipante, Classification and characterization of microsatellite instability across 18 cancer types, Nat. Med. 22 (2016) 1342–1350, https://doi.org/10.1038/nm.4191.
[10] Durham J.N. Le DT, K.N. Smith, H. Wang, B.R. Bartlett, L.K. Aulakh, et al., Mismatch repair deficiency predicts response of solid tumors to PD-1 blockade, Science 357 (2017) 409–413, https://doi.org/10.1126/science.aan6733.
[11] T.N. Schumacher, P.D. Schreiber, Neoantigens in cancer immunotherapy, Science 348 (2015) 69–74, https://doi.org/10.1126/science.aaa4971.
[12] T. Nagashima, Y. Shimoda, T. Tanabe, A. Naruoka, J. Saito, M. Serizawa, et al., Optimizing an ion semiconductor sequencing data analysis method to identify somatic mutations in the genomes of cancer cells in clinical tissue samples, Biomed. Res. 37 (2016) 359–366, https://doi.org/10.2220/biomedres.37.359.
[13] Y. Shimoda, T. Nagashima, K. Urakami, T. Tanabe, J. Saito, A. Naruoka, et al., Biomed. Res. 37 (2016) 367–379, https://doi.org/10.2220/biomedres.37.367.
[14] Y. Akiyama, R. Kondou, A. Iizuka, K. Ohshima, K. Urakami, T. Nagashima, et al., Immune response-associated gene analysis of 1,000 cancer patients using whole-exome sequencing and gene expression profiling-Project HOPE, Biomed. Res. 37 (2016) 233–242, https://doi.org/10.2220/biomedres.37.233.
[15] K. Ohshima, K. Hatakeyama, T. Nagashima, Y. Watanabe, K. Kanto, Y. Doi, et al., Integrated analysis of gene expression and copy number identified potential cancer driver genes with amplification-dependent overexpression in 1,454 solid tumors, Sci. Rep. 7 (641) (2017), https://doi.org/10.1038/s41598-017-00219-3.
[16] Y. Kiyohara, S. Yoshikawa, M. Otsuka, R. Kondou, A. Iizuka, C. Nonomura, et al., Melanoma patient response to nivolumab treatment for metastatic lung lesion : Multi-OMICS analysis in Project HOPE, J. Dermatol. 55 (2017) 1156–1159, https://doi.org/10.1111/1346-8138.13879.
[17] Y. Akiyama, M. Komiyama, Y. Nakamura, A. Iizuka, C. Oshita, A. Kume, et al., Identification of novel MAGE-A6- and MAGE-A12-derived HLA-A24-restricted cytotoxic T lymphocyte epitopes using an in silico peptide-docking assay, Cancer Immunol. Immunother. 61 (2012) 2311–2319, https://doi.org/10.1007/s00262-012-1298-1.
[18] Uram J.N. Le DT, H. Wang, B.R. Bartlett, H. Kemberling, A.D. Eyring, et al., PD-1 blockade in tumors with mismatch-repair deficiency, N. Engl. J. Med. 372 (2015) 2509–2520, https://doi.org/10.1056/NEJMoa1500596.
[19] M.S. Rooney, S.A. Shukla, C.J. Wu, G. Getz, N. Hacohen, Molecular and genetic

properties of tumors associated with local immune cytolytic activity, Cell 160 (2015) 48–61, https://doi.org/10.1016/j.cell.2014.12.033.
[20] C.Y. Ock, B. Keam, S. Kim, J.S. Lee, M. Kim, T.M. Kim, et al., Pan-cancer immunogenic perspective on the tumor microenvironment based on PD-L1 and CD8 T-cell infiltration, Clin. Cancer Res. 22 (2016) 2261–2270, https://doi.org/10.1158/1078-0432.CCR-15-2834.
[21] M.M. Gubin, X. Zhang, H. Schuster, E. Caron, J.P. Ward, T. Noguchi, et al., Checkpoint blockade cancer immunotherapy targets tumour-specific mutant antigens, Nature 515 (2014) 577–581, https://doi.org/10.1038/nature13988.
[22] E.M. Verdegaal, N.F. de Miranda, M. Visser, T. Harryvan, M.M. van Buuren, R.S. Andersen, et al., Neoantigen landscape dynamics during human melanoma-T cell interactions, Nature 536 (2016) 91–95, https://doi.org/10.1038/nature18945.
[23] S. Turajlic, K. Litchfield, H. Xu, R. Rosenthal, N. McGranahan, J.L. Reading, et al., Insertion-and-deletion-derived tumour-specific neoantigens and the immunogenic phenotype: a pan-cancer analysis, Lancet Oncol. 18 (2017) 1009–1021, https://doi.org/10.1016/S1470-2045(17)30516-8.
[24] V.P. Balachandran, M. Luksza, J.N. Zhao, V. Makarov, J.A. Moral, R. Remark, et al., Identification of unique neoantigen qualifies in long-term survivors of pancreatic cancer, Nature 551 (2017) 512–516, https://doi.org/10.1038/nature24462.
[25] L.B. Alexandrov, S. Nik-Zainai, D.C. Wedge, S.A. Aparicio, S. Behjati, A.V. Biankin, et al., Signature of mutational processes in human cancer, Nature 500 (2013) 415–421, https://doi.org/10.1038/nature12477.
[26] F. Duan, J. Duitama, S. Al Seesi, C.M. Ayres, S.A. Corcelli, A.P. Pawashe, et al., Genomic and bioinformatic profiling of mutational neoepitopes reveals new rules to predict anticancer immunogenicity, J. Exp. Med. 211 (2014) 2231–2248, https://doi.org/10.1084/jem.20141308.
[27] Y.C. Lu, X. Yao, J.S. Crystal, Y.F. Li, M. El-Gamil, C. Gross, et al., Efficient identification of mutated cancer antigens recognized by T cells associated with durable tumor regressions, Clin. Cancer Res. 20 (2014) 3401–3410, https://doi.org/10.1158/1078-0432.CCR-14-0433.
[28] C.J. Cohen, J.J. Gartner, M. Horovitz-Fried, K. Shamalov, K. Trebska-McGowan, V.V. Bliskovsky, et al., Isolation of neoantigen-specific T cells from tumor and peripheral lymphocytes, J. Clin. Invest. 125 (2015) 3981–3991, https://doi.org/10.1172/JCI82416.
[29] C. Linnemann, M.M. van Buuren, L. Bies, E.M. Verdegaal, R. Schotte, J.J. Calis, et al., High-throughput epitope discovery reveals frequent recognition of neo-antigens by CD4+ T cells in human melanoma, Nat. Med. 21 (2015) 81–85, https://doi.org/10.1038/nm.3773.
[30] M. Yadav, S. Jhunjhunwala, Q.T. Phung, P. Lupardus, J. Tanguay, S. Bumbaca, et al., Predicting immunogenic tumour mutations by combining mass spectrometry and exome sequencing, Nature 515 (2014) 572–576, https://doi.org/10.1038/nature14001.
[31] S. Kalaora, E. Barnea, E. Merhavi-Shoham, N. Qutob, J.K. Teer, N. Shimony, et al., Use of HLA peptidomics and whole exome sequencing to identify human immunogenic neo-antigens, Oncotarget 7 (2016) 5110–5117, https://doi.org/10.18632/oncotarget.6960.
[32] V. Kochin, T. Kanaseki, S. Tokita, S. Miyamoto, Y. Shionoya, Y. Kikuchi, et al., HLA-A24 ligandome analysis of colon and lung cancer cells identifies a novel cancer-testis antigen and a neoantigen that elicits specific and strong CTL responses, Oncoimmunology 6 (2017) e1293214, , https://doi.org/10.1080/2162402X.2017.1293214.
[33] C. Phetsouphanh, J.J. Zaunders, A.D. Kelleher, Detecting antigen-specific T cell responses: from bulk populations to single cells, Int. J. Mol. Sci. 16 (2015) 18878–18893, https://doi.org/10.3390/ijms160818878.
[34] I. Tirosh, A.S. Venteicher, C. Hebert, L.E. Escalante, A.P. Patel, K. Yizhak, et al., Single-cell RNA-seq supports a developmental hierarchy in human oligodendroglioma, Nature 539 (2016) 309–313, https://doi.org/10.1038/nature20123.
[35] A.A. Eltahla, S. Rizzetto, M.R. Pirozyan, B.D. Betz-Stablein, V. Venturi, K. Kedzierska, et al., Linking the T cell receptor to the single cell transcriptome in antigen-specific human T cells, Immunol. Cell Biol. 94 (2016) 604–611, https://doi.org/10.1038/icb.2016.16.
[36] S. Afik, K.B. Yates, K. Bi, S. Darko, J. Godec, U. Gerdemann, et al., Targeted reconstruction of T cell receptor sequence from single cell RNA-seq links CDR3 length to T cell differentiation state, Nucleic Acids Res. 45 (2017) e148, https://doi.org/10.1093/nar/gkx615.
[37] Y.C. Lu, Z. Zheng, P.F. Robbins, E. Tran, T.D. Prickett, J.J. Gartner, et al., An efficient single-cell RNA-seq approach to identify neoantigen-specific T cell receptors, Mol. Ther. 26 (2018) 379–389, https://doi.org/10.1016/j.ymthe.2017.10.018.
[38] I. Tirosh, B. Izar, S.M. Prakadan, Wadsworth M.H. 2nd, D. Treacy, J.J. Trombetta, et al., Dissecting the multicellular ecosystem of metastatic melanoma by single-cell RNA-seq, Science 352 (2016) 189–196, https://doi.org/10.1126/science.aad0501.
[39] C. Zheng, L. Zheng, J.K. Yoo, H. Guo, Y. Zhang, X. Guo, et al., Landscape of infiltrating T cells in liver cancer revealed by single-cell sequencing, Cell 169 (2017) 1342–1356, https://doi.org/10.1016/j.cell.2017.05.035.
[40] X. Guo, Y. Zhang, L. Zheng, C. Zheng, J. Song, Q. Zhang, et al., Global characterization of T cells in non-small-cell lung cancer by single-cell sequencing, Nat. Med. 27 (2018) 978–985, https://doi.org/10.1038/s41591-018-0045-3.
[41] J.J. Perry, G.D. Ballard, A.E. Albert, L.E. Dobrolecki, L.H. Malkas, D.J. Hoelz, Human C6orf211 encodes Armt1, a protein carboxyl methyltransferase that targets PCNA and is linked to the DNA damage response, Cell Rep. 10 (2015) 1288–1296, https://doi.org/10.1016/j.celrep.2015.01.054.
[42] A.K. Dunbier, H. Anderson, Z. Ghazoui, E. Lopez-Knowles, S. Pancholi, R. Ribas, et al., ESR1 is co-expressed with closely adjacent uncharacterized genes spanning a breast cancer susceptibility locus at 6q25.1, PLoS Genet. 7 (2011) e1001382, , https://doi.org/10.1371/journal.pgen.1001382.